

Quantum Data Bus in Dipolar Coupled Nuclear Spin Qubits

Jingfu Zhang,¹ Michael Ditty,¹ Daniel Burgarth,² Colm A. Ryan,¹ C. M. Chandrashekar,^{1,3}

Martin Laforest,¹ Osama Moussa,¹ Jonathan Baugh,¹ and Raymond Laflamme^{1,3}

¹*Institute for Quantum Computing and Department of Physics,*

University of Waterloo, Waterloo, Ontario, Canada N2L 3G1

²*IMS and QOLS, Imperial College, London SW7 2BK, UK*

³*Perimeter Institute for Theoretical Physics, Waterloo, Ontario, N2J 2W9, Canada*

(Dated: June 21, 2024)

Abstract

We implement an iterative quantum state transfer exploiting the natural dipolar couplings in a spin chain of a liquid crystal NMR system. During each iteration a finite part of the amplitude of the state is transferred and by applying an external operation on only the last two spins the transferred state is made to accumulate on the spin at the end point. The transfer fidelity reaches one asymptotically through increasing the number of iterations. We also implement the inverted version of the scheme which can transfer an arbitrary state from the end point to any other position of the chain and entangle any pair of spins in the chain, acting as a full quantum data bus.

PACS numbers: 03.67.Lx

In quantum computation and quantum communication the transfer of an arbitrary quantum state from one qubit to another is a fundamental element. The most obvious method to implement quantum state transfer (QST) on an array of qubits is based on a sequence of SWAP gates for neighboring spins. In spin qubit systems the SWAP gate can be implemented through the evolution of the dipolar coupling between the neighboring spins for $1/2D$ time by decoupling the other spins, where D denotes the dipolar coupling strength. In experiments, however, the required decoupling operations are hard to implement if the spins cannot be individually addressed by spectral selectivity, e.g., in large size solid NMR systems. This makes the direct implementation of such gates in a large spin system challenging.

To overcome this problem, schemes based on "always on" spin systems were proposed [1, 2]. The state can be transferred with unit fidelity in engineered spin chains or networks with XY interactions [3]. However, the required fine-tuned XY couplings are not found in natural spin systems [4]. In other schemes based on spin chains with Heisenberg interactions [1, 5] or with a double-quantum Hamiltonian [4], the fidelity of the QST cannot approach unity in scalable systems.

The above limitations can be relaxed significantly by applying gate operations to receive and store the transferred state [6, 7]. The gates are only applied to two spins at one end of a spin chain. In this Letter, we experimentally implement the QST in a liquid crystal NMR system based on this scheme. Opposed to previous experimental implementations [7], the dipolar couplings exist naturally in the system and are directly exploited for the QST. The transfer with high fidelity is achieved in an iterative manner. Each iteration transfers a finite part of the input amplitude to the target spin at the end of the chain. The fidelity of the transfer asymptotically approaches unity by increasing the number of iterations. We also experimentally demonstrate the time-inverted version of [6]. Through this, a full *quantum data bus* is implemented, where arbitrary unknown quantum states can be steered to an *any* position of the chain. This is also useful for the selective excitation of one spin, which is addressed by the two-spin gates, rather than by its individual properties, e.g. chemical shift in NMR. As opposed to previous schemes [8], global control is not required. Surprisingly the reversal operation can also be used to *entangle* any pair of spins in the chain by operations at its end only. We demonstrate the entangling operation in the qubits at the end points of the chain.

The QST and its reversal operations mean that the chain is really used as a wire with

an input, an output, and no gates in the middle, and only the many-body Hamiltonian of the chain is responsible for the transport. The required number of gates to achieve a good fidelity (e.g. larger than 0.9) scales roughly linearly with the system size [6]. Hence our method is scalable and suitable for large-size systems, such as solid or liquid crystal NMR systems, where the differences of the chemical shifts are too small to address the spins.

Our first goal is to transfer the state $\alpha|0\rangle + \beta|1\rangle$ from spins j to N in a N -spin chain. The Hamiltonian for spins 1 to $N - 1$ is represented as

$$H = \frac{1}{2}\pi \sum_{j,k=1; k>j}^{N-1} D_{jk}(2\sigma_z^j\sigma_z^k - \sigma_x^j\sigma_x^k - \sigma_y^j\sigma_y^k), \quad (1)$$

where σ_x^j , σ_y^j and σ_z^j denote the Pauli matrices with j indicating the affected spin. Noting that H preserves the total number of excited spins [1, 3], we have $U_\tau|\mathbf{0}\rangle = e^{i\theta}|\mathbf{0}\rangle$ and

$$U_\tau|\mathbf{j}\rangle = \sum_{k=1}^{N-1} a_k|\mathbf{k}\rangle. \quad (2)$$

Here $U_\tau = e^{-i\tau H}$ and $e^{i\theta}$ is the $(1, 1)$ matrix element of U_τ . The state $|\mathbf{0}\rangle$ denotes all spins pointing up, and $|\mathbf{j}\rangle$ denotes all spins up except the spin j pointing down.

The main operation is the two-spin gate applied only on spins $N - 1$ and N , and in iteration n the gate is denoted as

$$W(c_n, d_n) = I_{1,2,\dots,N-2} \otimes \begin{pmatrix} 1 & 0 & 0 & 0 \\ 0 & d_n^* & c_n^* & 0 \\ 0 & -c_n & d_n & 0 \\ 0 & 0 & 0 & 1 \end{pmatrix}_{N-1,N} \quad (3)$$

where $I_{1,2,\dots,N-2}$ denotes the unit operator for spins 1 to $N - 2$. The basis order for spins $N - 1$ and N is $|00\rangle$, $|01\rangle$, $|10\rangle$ and $|11\rangle$. It is straightforward to show that $W(c_n, d_n)(c_n|\mathbf{N} - \mathbf{1}\rangle + d_n|\mathbf{N}\rangle) = |\mathbf{N}\rangle$, noting that $|c_n|^2 + |d_n|^2 = 1$.

The N spin system is initialized into the input state $\alpha|\mathbf{0}\rangle + \beta|\mathbf{j}\rangle$ by setting spin j in the system to state $\alpha|0\rangle + \beta|1\rangle$. Here j is the location of the sender (receiver) of the QST for the (inverse) protocol, which is on some arbitrary spin of the quantum data bus. It is sufficient to only discuss the transfer of $|\psi_0\rangle = |\mathbf{j}\rangle$ because U_τ only introduces a known phase factor before $|\mathbf{0}\rangle$ and W does not change $|\mathbf{0}\rangle$. Iteration n is represented as

$$Q_{\mathbf{j},n} = [I_{1,2,\dots,N-2} \otimes W(c_n, d_n)][U_\tau \otimes I_N]. \quad (4)$$

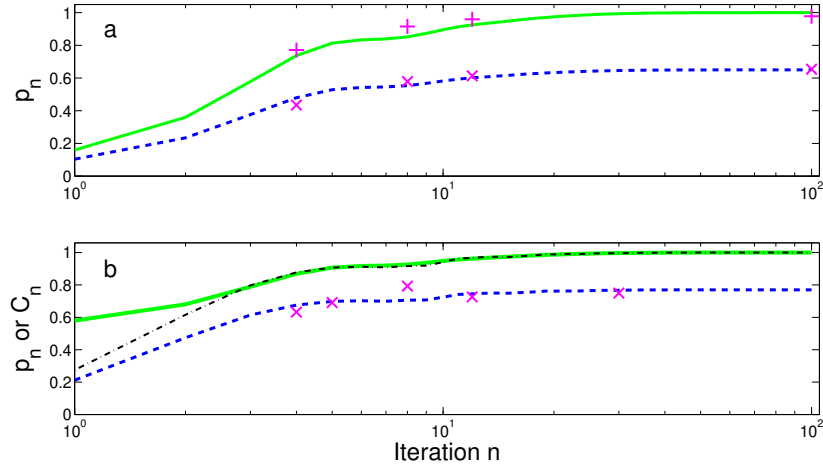


FIG. 1: (Color online) The numerical simulation (solid) and experimental results (data marked by "x" and "+") for the probability p_n of the QST as a function of iterations in the four spin system used in experiments (see text for dipolar couplings) for transferring a state from spins 1 to 4 (a) and entangling the two spins (b) when $\tau = 2.1$ ms. In figure (b) p_n can be approximated as the observable coherence C_n [dot-dashed, see Eq. (10)] when $n > 2$. The experimental data can be fitted as $0.65p_n$ and $0.77C_n$, shown as the dashed curves, respectively. The data marked by "+" show the probability after normalizing the measured $A_{k,n}$.

Using Eqs. (2-4), one can obtain the state in an iterative manner

$$|\psi_{n+1}\rangle = Q_{\mathbf{j},n+1}|\psi_n\rangle = \sum_{k=1}^N A_{k,n+1}|\mathbf{k}\rangle \quad (5)$$

Here $A_{N-1,n+1} = 0$, $A_{N,n+1} = \sqrt{p_{n+1}}$ where $p_0 = 0$ and $p_{n+1} = p_n + |\langle \mathbf{N} - \mathbf{1} | U_\tau \otimes I_N | \psi_n \rangle|^2$, $d_{n+1} = e^{i\theta} \sqrt{p_n} / \sqrt{p_{n+1}}$ and $c_{n+1} = \langle \mathbf{N} - \mathbf{1} | U_\tau \otimes I_N | \psi_n \rangle / \sqrt{p_{n+1}}$. In strict nearest-neighbour chains it can be shown [6] that p_n converges to unity by increasing the number of iterations. In the present case we have also non-nearest neighbour interactions, but numerical results show p_n still approaches unity, with a convergence speed which depends on the evolution time τ . [See Figure 1 (a)]. The process of QST after a large number of iterations can be presented as

$$T_{\mathbf{j},n}(\alpha|0\rangle + \beta|\mathbf{j}\rangle) \rightarrow \alpha e^{in\theta}|0\rangle + \beta|\mathbf{N}\rangle, \quad (6)$$

i.e., spin N ends with the state $\alpha e^{in\theta}|0\rangle + \beta|1\rangle$ and $e^{in\theta}$ is known, where

$$T_{\mathbf{j},n} = Q_{\mathbf{j},n} \dots Q_{\mathbf{j},2} Q_{\mathbf{j},1}. \quad (7)$$

We can exploit the inversion of $T_{\mathbf{j},n}$ to implement the QST from spin N to spin j , i.e., without applying the external operation directly on the spin j to evolve it into state $\alpha|0\rangle + \beta|1\rangle$. Hence the spin chain functions as a *quantum data bus*, which can transfer arbitrary unknown states to any qubit. This method also allows to create a selective excitation that does not require spectral selectivity, e.g. chemical shift in NMR, to address spin j . The external operations are only applied to spins $N - 1$ and N . From Eqs. (5) and (7) one finds

$$p_n = |\langle\psi_0|T_{\mathbf{j},n}^{-1}|\mathbf{N}\rangle|^2, \quad (8)$$

i.e., p_n is the fidelity for generating $|\psi_0\rangle$ by applying $T_{\mathbf{n},j}^{-1}$ to $|\mathbf{N}\rangle$. By modifying the input state one can obtain $T_{\mathbf{j},n}^{-1}(\alpha e^{i\theta}|\mathbf{0}\rangle + \beta|\mathbf{N}\rangle) \rightarrow \alpha|\mathbf{0}\rangle + \beta|\mathbf{j}\rangle$ [9].

The method of inverse QST furthermore can be used to entangle arbitrary spins j, k indirectly by acting at spins $N - 1$ and N only. This can be done by designing a pulse analogously to Eq. (4) through setting $|\psi_0\rangle = |\psi_{jk}\rangle = (|\mathbf{j}\rangle + |\mathbf{k}\rangle)/\sqrt{2}$ and replacing p_0 as $p_0 = |\langle\mathbf{N}|\psi_{jk}\rangle|^2$. The process is represented as

$$T_{\mathbf{j},\mathbf{k},n}|\psi_{jk}\rangle \rightarrow |\mathbf{N}\rangle, \quad (9)$$

and applying $T_{\mathbf{j},\mathbf{k},n}^{-1}$ on $|\mathbf{N}\rangle$. The required pulse sequence is very similar to the inverse QST. The fidelity for generating $|\psi_{jk}\rangle$ is also represented by Eq. (8) through replacing $T_{\mathbf{j},n}^{-1}$ by $T_{\mathbf{j},\mathbf{k},n}^{-1}$. The numerical simulation for p_n is illustrated as Figure 1 (b).

We use the four protons in ortho- chlorobromobenzene ($\text{C}_6\text{H}_4\text{ClBr}$) dissolved in the liquid crystal solvent ZLI-1132 as four qubits to implement the experiments. Using Cory48 [10] and 1-D MREV-8 pulse sequences and referring to the spectra of molecules with similar structures [11], we obtain the Hamiltonian of the spin system by fitting the spectra. The chemical shifts are measured to be 106.2, -187.7 , -58.6 , 91.3 with respect to the transmitter frequency, dipolar couplings are $D_{12} = -1233.7$, $D_{13} = -149.4$, $D_{14} = -93.2$, $D_{23} = -716.0$, $D_{24} = -236.6$, $D_{34} = -1677.5$ Hz, and the effective transverse relaxation times (T_2^*) for the four protons are 91, 87, 88 and 82 ms. The NMR spectrum obtained by Cory48 from the thermal equilibrium state $\rho_{th} = \sum_{i=1}^4 \sigma_z^i$ is shown in Figure 2 (a).

All experiments start with the deviation density matrix $\rho_{ini} = |0000\rangle\langle 0000| - |1111\rangle\langle 1111|$, which can be prepared by the double-quantum coherence Hamiltonian [12] $H_d = \frac{1}{2}\pi \sum_{k=2,j<k}^4 D_{jk}^d (\sigma_x^j \sigma_x^k - \sigma_y^j \sigma_y^k)$ in a molecule with C_{2v} symmetry [13]. However, we choose to generate the effective H_d using a GRadient Ascent Pulse Engineering pulse [14]. Using

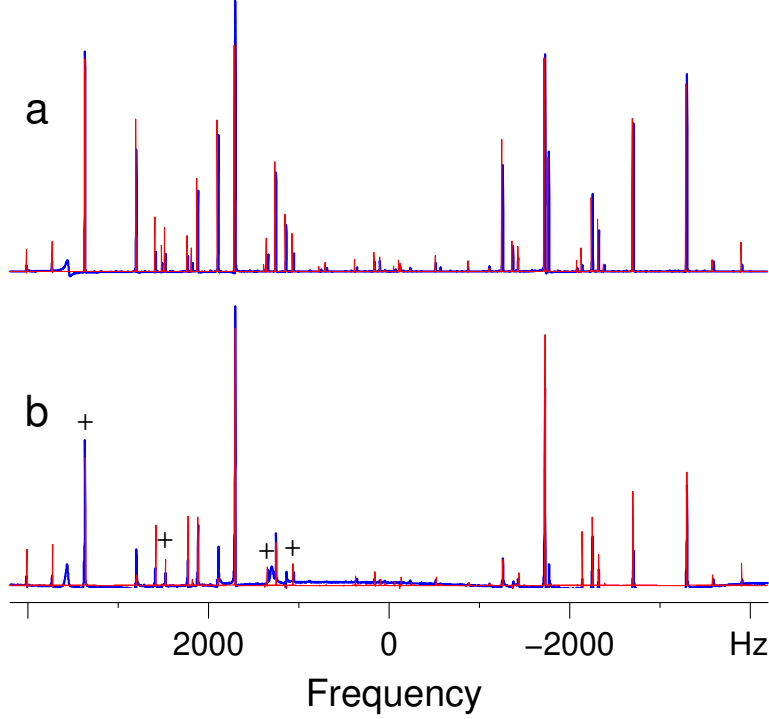


FIG. 2: (Color online) NMR spectra (blue thick) obtained by Cory48 pulse sequence from the thermal equilibrium state (a), and by a collective $\pi/2$ pulse from ρ_{ini} (b). The red thin spectra show the results by simulation. The plot's vertical axes have arbitrary units. The NMR peaks marked by "+" indicate the single-quantum transitions between magnetic quantum numbers 2 and 1.

temporal averaging, we prepare ρ_{ini} by summing the three states $U_d \rho_{th} U_d^\dagger$, $U_d^\dagger \rho_{th} U_d$, $2\rho_{th}$, where $U_d = e^{-it_d H_d}$ by choosing $t_d = 8.00/D_{12}^d$ [13]. In the numerical simulation we prepare ρ_{ini} with fidelity 99.97%. Figure 2 (b) shows the NMR spectrum obtained by a collective $\pi/2$ pulse in experiment when the system lies in ρ_{ini} . The NMR peaks marked by "+" indicate the single-quantum transitions between magnetic quantum numbers 2 and 1.

We demonstrate the QST by transferring ρ_0 from spins 1 to 4 by choosing $\rho_0 = \sigma_x$, σ_y , σ_z and I , respectively. Because $T_{j,n}$ is spin-preserving, the transitions marked by "+" in Figure 2 (b) can represent the QST starting with the input state $\rho_0|000\rangle\langle 000|$. We therefore can ignore $|1111\rangle\langle 1111|$ in ρ_{ini} and omit the negative frequency spectral region.

The input state is prepared by applying an operation U_{ini} to ρ_{ini} . With increasing n , $T_{1,n}$ transforms $\rho_0|000\rangle\langle 000|$ to $|000\rangle\langle 000|\rho$ asymptotically, where $\rho = e^{in\theta\sigma_z/2}\rho_0 e^{-in\theta\sigma_z/2}$. In experiments we removed the phase factor between ρ and ρ_0 by phase correction. For a fixed

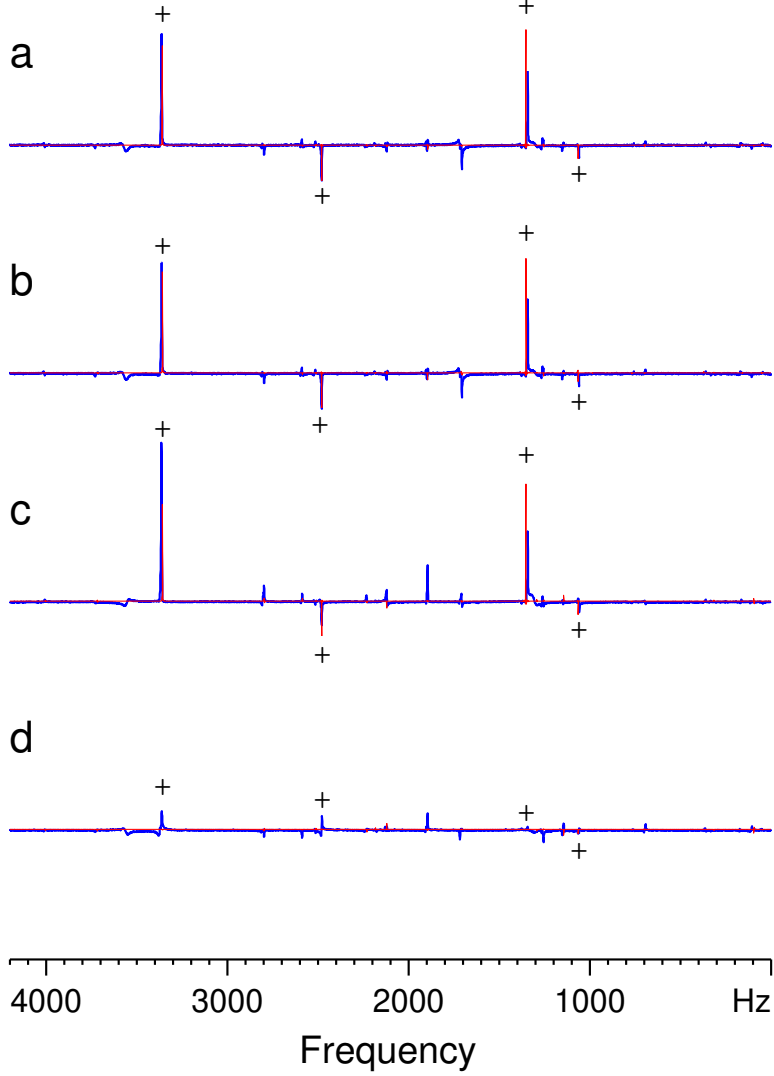


FIG. 3: (Color online) NMR spectra (a-d) for implementing the QST from spins 1 to 4 after 100 iterations, when the input states are chosen as $\sigma_x|000\rangle\langle 000|$, $\sigma_y|000\rangle\langle 000|$, $\sigma_z|000\rangle\langle 000|$ and $I|000\rangle\langle 000|$ respectively, where the readout operation $e^{i\pi\sigma_y^4/4}$ is applied to obtain observable signals in (c) or (d). The plot's vertical axes have the same scale.

n , we implement the unitary $T_{1,n}U_{ini}$ using one GRAPE pulse. The experimental results of the QST after 100 iterations for the various input states are shown as Figures 3 (a-d), respectively.

Exploiting the transformation between the computational basis and energy eigenbasis, and ignoring the difference of T_2^* of the four protons, we can approximatively obtain $A_{k,n}$ in Eq. (5) through measuring the amplitudes of the peaks marked by "+" in Figures 3 (a-c) by choosing the signals in Figure 2 (b) as the reference. Therefore we obtain $p_n =$

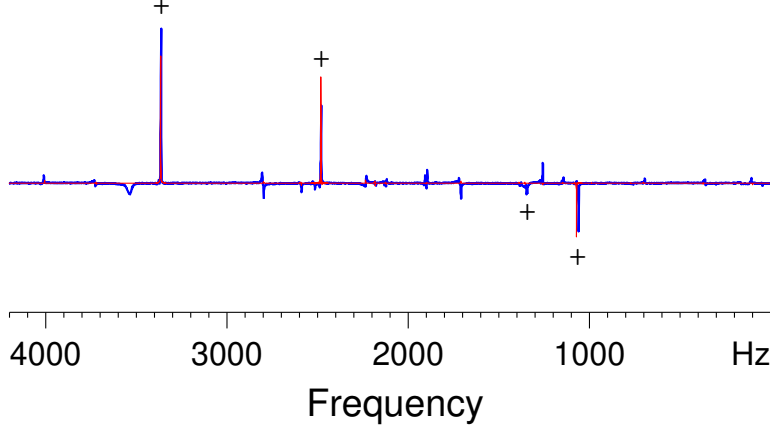


FIG. 4: (Color online) NMR spectra for implementing the selective excitation and quantum data bus for spin 2.

$|A_{4,n}|^2$. For the input states $\sigma_x|000\rangle\langle 000|$, $\sigma_y|000\rangle\langle 000|$, $\sigma_z|000\rangle\langle 000|$, p_{100} is measured as 0.654 ± 0.046 , 0.660 ± 0.052 and 0.693 ± 0.037 , respectively. All other $|A_{k,100}|^2$ are below 0.02. After normalizing the measured $A_{k,100}$, i.e., ignoring the decay of the signals during the transfer, we obtain the transfer probability represented as 0.978 ± 0.018 , 0.973 ± 0.026 and 0.989 ± 0.001 corresponding to the three input states, respectively. The perfect state transfer is demonstrated up to decay of signals.

To observe p_n increasing with n , we also implement the QST by choosing various n when the input state is $\sigma_x|000\rangle\langle 000|$. The measured p_n is shown as the data marked by "x" in Figure 1 (a). The experimental data can be fitted as $0.65p_n$. The probability after normalization is shown as the data marked by "+".

Next we implement the selective excitation / quantum data bus for spin 2. The reverse QST starts with the input state $|000\rangle\langle 000|\sigma_x$ obtained by applying $R_y^4 = e^{-i\sigma_y^4\pi/4}$ to ρ_{ini} . When $n = 100$, $T_{2,n}^{-1}$ transforms $|000\rangle\langle 000|\sigma_x$ to $|0\rangle\langle 0|\rho|00\rangle\langle 00|$ with probability close to 1, where $\rho = e^{-in\theta\sigma_z/2}\sigma_x e^{in\theta\sigma_z/2}$. The experimental results are shown in Figure 4. The fidelity of excitation is measured as 0.744 ± 0.036 , and 0.973 ± 0.009 after normalization.

We choose $|\psi_{14}\rangle = (|1\rangle + |4\rangle)/\sqrt{2}$ as the target to demonstrate the entangling operation in spins 1 and 4. To measure the fidelity, we rewrite Eq. (8) as $p_n = |\langle 0000|\Psi_n\rangle|^2$ [15]. Here $|\Psi_n\rangle = P^\dagger T_{1,4,n}^{-1}|\mathbf{4}\rangle$ where P denotes the operation to prepare $|\psi_{14}\rangle$ from $|0000\rangle$ (e.g. see [16]). When p_n is close to 1, we can obtain p_n approximately by applying a readout operation $e^{i\pi\sigma_y^1/4}$ to $|\Psi_n\rangle$. Noting that $|1111\rangle\langle 1111|$ in ρ_{ini} does not contribute observable

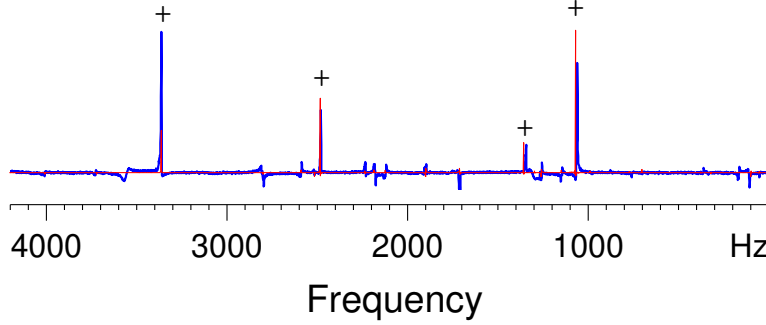


FIG. 5: (Color online) NMR spectra for measuring the fidelity of the generation of $(|1\rangle + |4\rangle)/\sqrt{2}$.

signals for measuring p_n , we approximate p_n as the coherence

$$C_n = \text{Tr}(2|0000\rangle\langle 1000|\rho_n) \quad (10)$$

where $\rho_n = U_{tot,n}\rho_{ini}U_{tot,n}^\dagger$ with $U_{tot,n} = e^{i\pi\sigma_y^1/4}P^\dagger T_{1,4,n}^{-1}e^{i\pi\sigma_x^4/2}$. The numerical simulation for C_n is shown in Figure 1 (b), where $|C_n - p_n| \leq 0.0175$ when $n > 2$. The measured C_n is shown in Figure 1 (b), where the experimental data can be fitted as $0.77C_n$. Figure 5 illustrates the NMR spectra when $n = 8$.

The operations U_d , U_d^\dagger , R_y^4 , $T_{1,n}U_{ini}$, $T_{2,n}^{-1}R_y^4$, and $U_{tot,n}$ are experimentally implemented using the GRAPE pulses with fidelities in theory larger than 0.99, respectively. The pulse lengths are 10 ms for U_d and U_d^\dagger , 20 ms for the other pulses. The experimental errors could mainly result from the inhomogeneities of the magnetic field, imperfection of GRAPE pulses and decoherence. In order to estimate the quality of the experimental spectra, we also list the ideal ones in simulation, shown as the red thin curves in Figures 2-5.

In conclusion, we have given an NMR implementation for various important tasks of quantum control that in principle can be achieved *indirectly* by controlling the end of a spin chain. Firstly, we implemented the transfer of an arbitrary quantum state. The dipolar couplings naturally existing in the liquid crystal NMR system are directly exploited for the QST. Our method is efficient and scalable in large size systems. Secondly, by implementing the reverse QST, we have created a full quantum data bus which is controlled by the two-qubit end gates. Finally as another application of the reverse QST, we proposed and demonstrated a new method to implement an entangling operation.

We thank D. Cory, C. Ramanathan, S. Bose, G. B. Furman and T. S. Mahesh for helpful discussions. We acknowledge support by the EPSRC grant EP/F043678/1, NSERC,

- [1] S. Bose, Phys. Rev. Lett. **91**, 207901 (2003).
- [2] S. Bose, Contemporary Physics **48**, 13 (2007); D. Burgarth, arXiv: 0704.1309 [quant-ph].
- [3] M. Christandl et al., Phys. Rev. Lett. **92**, 187902(2004); C. D. Franco, M. Paternostro, M. S. Kim, *ibid.* **101**, 230502 (2008).
- [4] P. Cappelaro, C. Ramanathan, and D. G. Cory, Phys. Rev. Lett. **99**, 250506 (2007).
- [5] E. B. Fel'dman and A. I. Zenchuk, arXiv:0809.1967v1 [quant-ph].
- [6] D. Burgarth, V. Giovannetti, S. Bose, Phys. Rev. A **75**, 062327 (2007).
- [7] J. Zhang et al., Phys. Rev. A **76**, 012317 (2007).
- [8] J. Fitzsimons and J. Twamley, Phys. Rev. Lett. **97**, 090502 (2006); J. Fitzsimons et al., *ibid.* **99**, 030501 (2007); P. Cappelaro, C. Ramanathan, and D. G. Cory, Phys. Rev. A **76**, 032317 (2007).
- [9] In our experimental system, we directly implemented the backward time evolution $U_{-\tau}$ of $Q_{\mathbf{j},n}^{-1}$ by forward evolution of $-H$. This is not necessary [2] but simplified the presentation. Actually one can design $Q_{\mathbf{j},n}$ in the Eq. (4) for the reverse QST using $-H$. Hence in the implementation of $Q_{\mathbf{j},n}^{-1}$ the evolution is still U_{τ} .
- [10] D. G. Cory, J. B. Miller, and A. N. Garroway, J. Magn. Reson. **90**, 205 (1990).
- [11] M. K. Henry et al., Phys. Rev. Lett. **99**, 220501 (2007); T. S. Mahesh and D. Suter, Phys. Rev. A **74**, 062312 (2006).
- [12] J. Baum et al., J. Chem. Phys. **83** 2015 (1985); J.-S. Lee and A. K. Khitrin, Phys. Rev. A **70**, 022330 (2004); J. Chem. Phys. **121**, 3949 (2004).
- [13] G. B. Furman, J. Phys. A **39**, 15197 (2006).
- [14] J. Baugh et al., Phys. in Can. **63**, No. 4 (2007), "Special issue on quantum information and quantum computing"; N. Khaneja et al., J. Magn. Reson. **172**, 296 (2005); C.A. Ryan et al., Phys. Rev. A **78**, 012328 (2008).
- [15] J. Zhang et al., Phys. Rev. A **79**, 012305 (2009).
- [16] I. L. Chuang et al., Proc. R. Soc. London, Ser. A **454**, 447 (1998).